

Figure 1. Proton decoupled solid-state ^{13}C cross-polarization spectra at 14.19 MHz of (A) praseodymium acetate, nonspinning; (B) praseodymium acetate, magic angle spinning at 2.7 kHz; (C) praseodymium acetate, magic angle spinning at 4.5 kHz; and (D) lanthanum acetate, magic angle spinning at 2.7 kHz. The expected positions of the spinning sidebands are indicated.

to spinning sidebands. The expected positions of the first- and second-order spinning sidebands are marked by stick diagrams below the spectra. The lines at 66 and 28 ppm have no observable sidebands.

From the chemical composition of praseodymium acetate one expects two ^{13}C resonances, one for the methyl group and the other for the carboxylate group. In aqueous solution two ^{13}C resonance lines are observed, one at 174.4 ppm and the other at 45.5 ppm. The CP-MAS spectra suggest the possibility that two chemically nonequivalent acetate ions may be present in the crystal. To the best of our knowledge the crystal structure of praseodymium acetate is unavailable. However, a detailed structural study has been reported⁶ for the trifluoroacetate analogue, where two different types of trifluoroacetate groups are reported. Of the four resonances observed in the solid state it is reasonable to assign the 211 and 114 ppm lines to carboxylate groups, on the basis of the very large chemical shift anisotropy observed. This large shift difference (97 ppm) must arise from the paramagnetic shielding anisotropy. The difference between the isotropic shifts of the remaining two resonances, presumably arising from the methyl groups of nonequivalent acetate ions, is much smaller (~ 38 ppm). From the relative intensities of the spinning side bands and the low-field portion of the nonspinning spectrum it appears that the carboxylate carbon with the isotropic shift of 211 ppm has considerably larger chemical shift anisotropy than the one at 114 ppm. A more detailed analysis is in progress.

The high-speed spinning spectra of praseodymium acetate, lanthanum acetate, and the solution-state spectra of both indicate that (1) high resolution in the solid is not only possible for the paramagnetic compound but very good, (2) the chemical shifts for the resonances in the paramagnetic solid are not identical with those in the solution case, and (3) this difference is due to the paramagnetism of the praseodymium ion. We have also investigated the NMR spectra of several other ligands and paramagnetic ions. In some cases the resonances of carbon atoms closest to the metal center are unobservable, in other cases the electron relaxation rate of the lanthanide ion in the solid is sufficiently slow that all resonances are very broad or even unobservable. However, praseodymium is not unique in providing usable spectra. Spectral parameters are compared for several acetates in Table I.

(6) Bone, S. P.; Sowerby, D. B.; Verma, R. D. *J. Chem. Soc. Dalton Trans.* 1978, 1544-1548.

Table I. Carbon-13 Chemical Shifts in Lanthanide Acetates^a

	carboxyl		methyl	
	liquid	solid	liquid	solid
La ³⁺	185.1	185	23.9	23
Pr ³⁺	174.4	211 114	45.5	66 28
Eu ³⁺	253.3		25.7	-47

^a ppm with respect to external Me₄Si. Here liquid-state shifts were measured in saturated solutions in $^2\text{H}_2\text{O}$ at ambient temperature.

The chemical shift dispersion gained in the paramagnetic complex may not appear very great when compared with the increase in line width observed at this magnetic field strength. However, the absence of molecular tumbling to modulate the chemical shift anisotropy in the solid should eliminate the usual broadening associated with a paramagnetic shift reagent at higher magnetic field strengths, which limits to some extent their utility in solution-phase studies. Thus, the 35-ppm line width for the methyl resonance of the europium compound will probably drop to 7 ppm or less in a 300-MHz proton field, making the shift 10 times the broadening. It should be noted that for an electron-nuclear dipolar interaction modified by the anisotropy of the g factor and zero-field splittings,⁷ the axis of quantization of the electron magnetization will be tipped away from the nuclear Zeeman direction. Fortunately however, a very short electron T_1 should average the electron nuclear dipole-dipole interaction considerably. Mechanical spinning may not eliminate all the residual inhomogeneous broadening because, as in the case of coupling to quadrupole nuclei,⁵ the magic angle directions for the electron and nucleus may differ. The resolution cannot improve without bound, however, since increasing the magnetic field strength may be accompanied by an increase in the electron T_1 .

Acknowledgment. This work was supported by the National Institutes of Health (GM-29428).

Registry No. Praseodymium acetate, 6192-12-7; europium acetate, 1184-63-0.

(7) Jesson, J. P. In "NMR of Paramagnetic Molecules—Principles and Applications"; LaMar, G. N., Horrocks, W. DeW., Jr., Holm, R. H., Eds.; Academic Press: New York, 1973; p 35.

Metal-Metal Interactions in Binuclear Platinum(II) Diphosphite Complexes. Resonance Raman Spectra of the $^1\text{A}_{1g}(\text{d}\sigma^*)^2$ and $^3\text{A}_{2u}(\text{d}\sigma^*\text{p}\sigma)$ Electronic States of $\text{Pt}_2(\text{P}_2\text{O}_5\text{H}_2)_4^{4-}$

Chi-Ming Che,^{1a} Leslie G. Butler,^{1a} Harry B. Gray,^{*1a}
R. M. Crooks,^{1b} and William H. Woodruff^{*1b}

Contribution No. 6819, Arthur Amos Noyes Laboratory
California Institute of Technology
Pasadena, California 91125
and Department of Chemistry
University of Texas at Austin
Austin, Texas 78712
Received April 1, 1983

Recent spectroscopic studies have established that certain binuclear $\text{d}^8\text{-d}^8$ complexes exhibit substantial metal-metal bonding interactions in their ground and lowest electronic excited states.²⁻⁸

(1) (a) California Institute of Technology. (b) University of Texas at Austin.

(2) Miskowski, V. M.; Nobinger, G. L.; Kliger, D. S.; Hammond, G. S.; Lewis, N. S.; Mann, K. R.; Gray, H. B. *J. Am. Chem. Soc.* 1978, 100, 485.

(3) Mann, K. R.; Gray, H. B. *Adv. Chem. Ser.* 1979, 173, 225.

(4) Rice, S. F.; Gray, H. B. *J. Am. Chem. Soc.* 1981, 103, 1593.

Table I. Structural and Spectroscopic Parameters for Binuclear Platinum and Rhodium Complexes

complex	state	$d(M-M)$, Å	$\nu(M-M)$, cm^{-1}	$k(M-M)$, mdyn Å^{-1}
$\text{Pt}_2(\text{pop})_4^{4-}$	$^1A_{1g}(d\sigma)^2(d\sigma^*)^2$	2.925 ^a	118	0.80
	$^3A_{2u}(d\sigma)^2(d\sigma^*p\sigma)$	2.71 ^b	156	1.40
$\text{Pt}_2(\text{pop})_4\text{Cl}_2^{4-}$	$^1A_{1g}(d\sigma)^2$	2.695 ^c	158 ^c	2.08
	$^3A_{2u}(d\sigma)^2(d\sigma^*)^2$	3.242 ^d	79 ^e	0.19
$\text{Rh}_2\text{b}_4^{2+}$	$^3A_{2u}(d\sigma)^2(d\sigma^*p\sigma)$	2.94 ^f	144 ^e	0.63
	$^1A_{1g}(d\sigma)^2$	2.837 ^g	134 ^h	0.95
$\text{Rh}_2\text{b}_4\text{Cl}_2^{2+}$	$^1A_{1g}(d\sigma)^2$	2.837 ^g	134 ^h	0.95
	$^3A_{2u}(d\sigma)^2(d\sigma^*)^2$	3.193 ⁱ	60 ^e	0.11
$[\text{Rh}(\text{CNPh})_4]_2^{2+}$	$^1A_{1g}(d\sigma)^2(d\sigma^*)^2$	3.193 ⁱ	60 ^e	0.11
	$^3A_{2u}(d\sigma)^2(d\sigma^*p\sigma)$		162 ^e	0.80

^a Reference 9. ^b Reference 8. ^c Che, C.-M.; Schaefer, W. P.; Gray, H. B.; Dickson, M. K.; Stein, P. B.; Roundhill, D. M. *J. Am. Chem. Soc.* **1982**, *104*, 4253. ^d Mann, K. R.; Thich, J. A.; Bell, R. A.; Coyle, C. L.; Gray, H. B. *Inorg. Chem.* **1980**, *19*, 2462. ^e Reference 5. ^f Reference 4. ^g Mann, K. R.; Bell, R. A.; Gray, H. B. *Inorg. Chem.* **1979**, *18*, 2671. ^h Miskowski, V. M.; Loehr, T. M.; Gray, H. B., to be submitted for publication. ⁱ Mann, K. R.; Lewis, N. S.; Williams, R. M.; Gray, H. B.; Gordon II, J. G. *Inorg. Chem.* **1978**, *17*, 828.

A useful model for Pt-Pt interactions of this sort is provided by the binuclear diphosphite-bridged complex, $\text{Pt}_2(\text{pop})_4^{4-}$ (pop = HOOPPOOH^{2-}).⁶⁻⁹ Vibronically resolved absorption and emission spectra of this complex suggest that its electronic properties are similar to those of several binuclear rhodium(I) species that have been studied extensively in our laboratories.⁸ Here we report the results of time-resolved resonance Raman (TR^3) spectroscopic measurements on $\text{Pt}_2(\text{pop})_4^{4-}$ that confirm that the Pt-Pt bonding in the $^3A_{2u}(d\sigma^*p\sigma)$ excited state is much stronger than that in the ground state.

Details of the TR^3 technique have been described previously.^{5,10} Aqueous solutions of $\text{Pt}_2(\text{pop})_4^{4-}$ (10^{-3} M) were deaerated prior to the Raman experiments. The laser excitation sources for the cw Raman and TR^3 experiments were the 356.4-nm line of a Spectra-Physics 171 Kr^+ laser and the 354.7-nm third harmonic of a Quanta-Ray DCR-1A Nd:YAG oscillator/amplifier, respectively. The transient absorption spectrum of the $^3A_{2u}(d\sigma^*p\sigma)$ state of $\text{Pt}_2(\text{pop})_4^{4-}$ exhibits an intense peak at 325 nm and a broad band at 400–500 nm.⁷ The 325-nm system has been assigned⁷ to the $d\sigma \rightarrow d\sigma^*$ transition of the $^3A_{2u}(d\sigma^*p\sigma)$ excited state of $\text{Pt}_2(\text{pop})_4^{4-}$. Excitation of $\text{Pt}_2(\text{pop})_4^{4-}$ at 354.7 nm results in fluorescence (410 nm, $^1A_{2u} \rightarrow ^1A_{1g}$; $\tau \leq 2$ ns) and phosphorescence (520 nm, $^3A_{2u} \rightarrow ^1A_{1g}$; $\tau \sim 10$ μs) with $I_{520} \gg I_{410}$.⁷ Thus, during our 7-ns Nd:YAG laser pulse, the major species present is the $^3A_{2u}(d\sigma^*p\sigma)$ state of $\text{Pt}_2(\text{pop})_4^{4-}$. Decay of this excited state to the ground state is complete in the 100 ms between laser pulses.

The $^1A_{1g}$ and $^3A_{2u}$ resonance Raman spectra of $\text{Pt}_2(\text{pop})_4^{4-}$ are shown in Figure 1. The ground-state spectrum (lower trace) shows an intense peak at 118 cm^{-1} with two evident overtones, whereas the excited-state TR^3 spectrum of the same solution (upper trace) exhibits an intense peak at 156 cm^{-1} with one overtone. The 118-cm^{-1} band is assigned to the Pt-Pt stretching motion of the $^1A_{1g}$ state of $\text{Pt}_2(\text{pop})_4^{4-}$ on the basis of its large enhancement in resonance with the $d\sigma^* \rightarrow p\sigma$ electronic transition and the overtone progression. The 156-cm^{-1} band is attributed to the excited-state ($^3d\sigma^*p\sigma$) Pt-Pt stretch. The fact that the intensity of the 156-cm^{-1} band relative to the 118-cm^{-1} ground-state peak increases as the laser pulse energy increases confirms our assignment. An examination of the overtones of the Pt-Pt stretch in the ground-state resonance Raman spectrum of $\text{Pt}_2(\text{pop})_4^{4-}$ shows small anharmonicity (ca. 1 cm^{-1} per progression member). The single overtone observed for $^3A_{2u}(d\sigma^*p\sigma)$ suggests similarly small anharmonicity in the excited state.

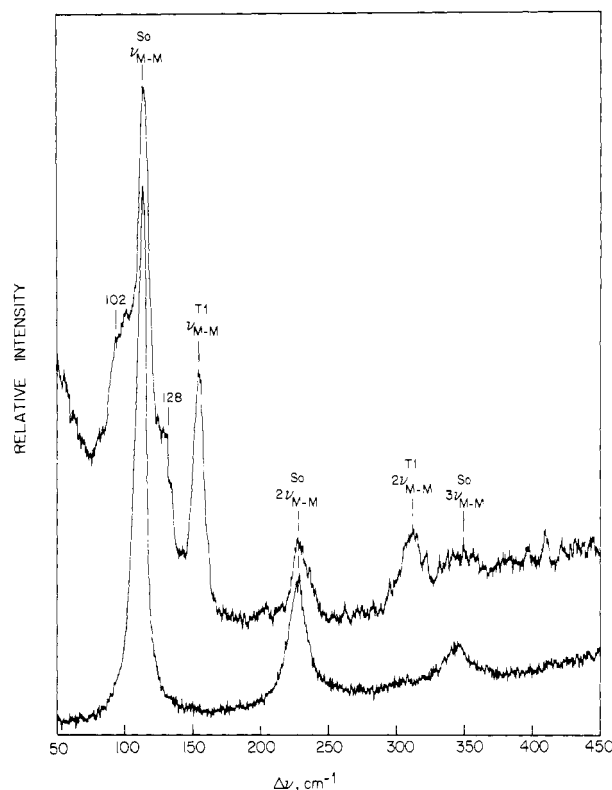


Figure 1. Lower trace: ground-state resonance Raman spectrum of $\text{Pt}_2(\text{pop})_4^{4-}$ obtained by continuous excitation at 356.4 nm. Upper trace: excited-state resonance Raman spectrum using pulsed Nd:YAG laser at 354.7 nm. So = $^1A_{1g}$; T1 = $^3A_{2u}$.

Shoulders at 102 and 128 cm^{-1} are evident on the 118-cm^{-1} ground-state peak (Figure 1). The intensity of the high-frequency shoulder follows the same dependence of intensity upon laser pulse energy exhibited by the 156-cm^{-1} excited-state peak, and therefore we infer that this is a low-energy mode of $^3A_{2u}(d\sigma^*p\sigma)$. The low-frequency shoulder is due to an unidentified thermal product peculiar to the high per-pulse energy excitation conditions of the TR^3 experiment.

The observed change in the Pt-Pt stretching frequency from 118 cm^{-1} ($^1A_{1g}$) to 156 cm^{-1} ($^3d\sigma^*p\sigma$) corresponds to a factor of 1.8 increase in the restoring force for this normal mode in the excited state relative to the ground state. For comparison, the M-M restoring force in the $^3d\sigma^*p\sigma$ excited state of $\text{Rb}_2\text{b}_4^{2+}$ ($b = 1,3$ -diisocyanopropane) increases by a factor of 3.3, whereas for $[\text{Rh}(\text{CNPh})_4]_2^{2+}$ the increase is a factor of 7.3 (Table I). Because of kinematic coupling between ligand modes and metal-metal stretching modes, comparisons of force constants among d^8 - d^8 species with different ligands necessarily include contributions from the restoring force of the ligand as well as the M-M bond and may not be meaningful. However, it is interesting to note that in the $^3d\sigma^*p\sigma$ excited state the binuclear platinum complex has the greatest restoring force for the M-M coordinate of the

(5) Dallinger, R. F.; Miskowski, V. M.; Gray, H. B.; Woodruff, W. H. *J. Am. Chem. Soc.* **1981**, *103*, 1595.

(6) Fordyce, W. A.; Brummer, J. G.; Crosby, G. A. *J. Am. Chem. Soc.* **1981**, *103*, 7061.

(7) Che, C.-M.; Butler, L. G.; Gray, H. B. *J. Am. Chem. Soc.* **1981**, *103*, 7796.

(8) Rice, S. F.; Gray, H. B. *J. Am. Chem. Soc.*, in press.

(9) (a) Filomena Dos Remedios Pinto, M. A.; Sadler, P. J.; Neidle, S.; Sanderson, M. R.; Subbiah, A.; Kuroda, R. *J. Chem. Soc., Chem. Commun.* **1980**, 13. (b) Che, C.-M.; Herbstein, F. H.; Schaefer, W. P.; Marsh, R. E.; Gray, H. B. *J. Am. Chem. Soc.*, in press. (c) Che, C.-M.; Butler, L. G.; Gray, H. G., to be submitted for publication.

(10) Dallinger, R. F.; Woodruff, W. H. *J. Am. Chem. Soc.* **1979**, *101*, 4391.

series,¹¹ and, in the ground state, it has a 4-fold greater restoring force than $Rh_2b_4^{2+}$.

The variation in metal-metal bond distances among the binuclear platinum and rhodium complexes is informative (Table I). We infer from the ~ 0.3 Å shorter ground-state M-M bond distance that diphosphite is substantially more constraining than the bridging isocyanide. As a result, the decrease in bond length upon excitation or oxidation is larger for $Rh_2b_4^{2+}$ than for $Pt_2(pop)_4^{4-}$. In each case, however, the structural and spectroscopic properties of the M-M bond in the triplet excited state closely approximate those of the corresponding dichloro ($d\sigma$)² d^7-d^7 species, thereby attesting to the utility of the ($d\sigma$)² ($d\sigma^*p\sigma$) (i.e., single M-M bond) formulation of $^3A_{2u}$. Important additional information about M-M interactions in these binuclear complexes should be obtained from studies now underway on the products of the excited-state electron-transfer quenching reactions.

Acknowledgment. We thank Vince Miskowski for helpful discussions. This research was supported by National Science Foundation Grants CHE81-20419 (C.-M.C., L.G.B., and H.B.G.) and CHE81-09541 (R.M.C. and W.H.W.).

(11) Another spectroscopic manifestation of the large Pt-Pt bond compression is the high energy (~ 3.8 eV)⁷ of the $d\sigma \rightarrow d\sigma^*$ transition in the $^3d\sigma^*p\sigma$ state of $Pt_2(pop)_4^{4-}$ relative to $Rh_2b_4^{2+}$ (~ 3 eV).²

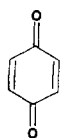
Synthesis of Conduritol A from Benzoquinone Using 9-[(Benzyloxy)methoxy]anthracene as a Protecting and Directing Group

Spencer Knapp,* Raphael M. Orna,¹ and Karen E. Rodrigues

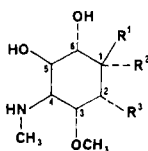
Department of Chemistry
Rutgers, The State University of New Jersey
New Brunswick, New Jersey 08903

Received March 28, 1983

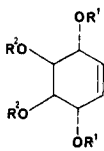
As part of our efforts² to synthesize aminocyclitol antibiotics³ from non-carbohydrate starting materials, we considered the conversion of benzoquinone (**1**) to the (\pm)-fortamines **2**.^{4,5} Compound **1** has carbonyl groups at C-3 and C-6 (fortimicin



1



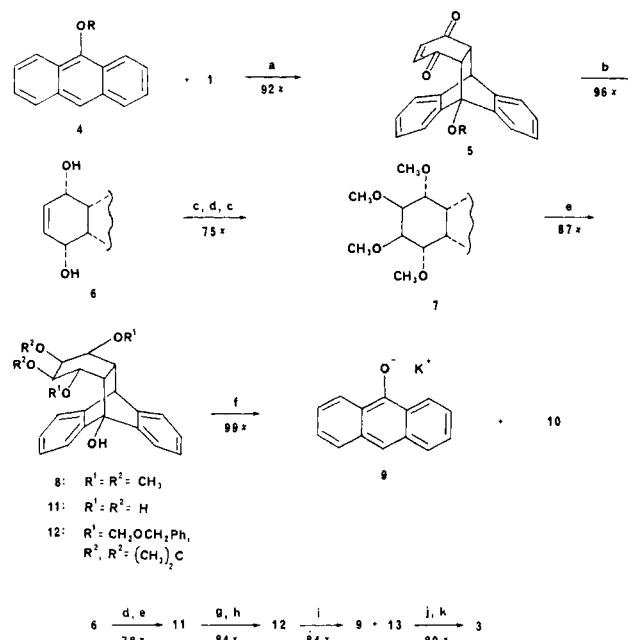
2a: $R^1 = NH_2$, $R^2 = H$, $R^3 = OH$
2b: $R^1 = NH_2$, $R^2 = H$, $R^3 = H$
2c: $R^1 = H$, $R^2 = NH_2$, $R^3 = H$



3: $R^1 = R^2 = H$
10: $R^1 = R^2 = CH_3$
13: $R^1 = CH_2OCH_2Ph$,
 $R^2, R^3 = (CH_3)_2C$

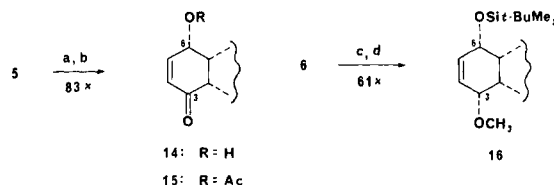
numbering), which might be reduced to the *cis*-3,6-dihydroxy functionality. Formal oxyamination and hydroamination of the C=C bonds of **1** would complete the functionalization. In order to implement these ideas we chose to preserve the enedione part structure of **1** by protecting one C=C bond. The protecting agent

Scheme I



^a Toluene, 68 °C, 15 h. ^b $NaBH_4$, $CeCl_3$, methanol, toluene, -78 °C. ^c CH_3I , NaH, THF. ^d OsO_4 , NMO, acetone, water. ^e TFA, methanol, 40 °C. ^f KH, dioxane, 25 °C, 2 h. ^g Acetone, TFA, 65 °C. ^h R^1Cl , NaH, THF. ⁱ KH, dioxane, 35 °C, 12 h. ^j Na, ammonia, ethanol, ether, -78 °C. ^k TFA, methanol.

Scheme II



^a Bu_4NBH_4 , dichloromethane, -78 °C. ^b Ac_2O , DMAP, pyridine, dichloromethane. ^c $t-BuMe_2SiOTf$, collidine, toluene, -100 °C. ^d CH_3I , KH, HMPA, THF, 0 °C.

would be maximally effective if it (a) protects one C=C bond of **1** without introducing any reactive functional groups, (b) blocks one face of **1** to direct *cis* reduction at C-3 and C-6 and *cis* functionalization of the remaining C=C bond, (c) allows the differentiation of the C-3 and C-6 hydroxyls, and (d) may be removed under mild conditions. We wish to describe a protecting group that meets all these needs and, coincidentally, enables the first stereospecific synthesis of the naturally occurring cyclitol conduritol A (**3**).^{6,7}

Reaction of **1** with 9-[(benzyloxy)methoxy]anthracene⁸ (**4**, Scheme I, $R = CH_2OCH_2Ph$) gave the adduct **5**, in which one C=C bond and one face of **1** are now protected from attack by reagents. In addition, the presence of the (benzyloxy)methoxy group near one carbonyl group (*pro*-C-3, say) offers a means to distinguish it from C-6. Sodium borohydride-cerium(III) chloride⁹ reduction of **5** at -78 °C gave the enediol **6**. The hydroxy groups were methylated, the remaining C=C bond was oxidized from the accessible face with osmium tetroxide,¹⁰ and the resulting diol was methylated to give the tetramethoxy compound **7**. This

(1) Louis Bevier Fellow, 1981-1982.

(2) For related work from our laboratory, see: Knapp, S.; Patel, D. V. *Tetrahedron Lett.* **1982**, 23, 3539.

(3) Rinehart, K. L.; Suami, T. "Aminocyclitol Antibiotics"; American Chemical Society: Washington, D.C., **1980**.

(4) Compounds **2a** (fortamine), **2b** (2-deoxyfortamine), and **2c** (2-deoxy-1-epifortamine) are the aminocyclitol portions of the antibiotics fortimicin A, istamycin A, and sporaricin A, respectively, among others. For isolation and structures see: (a) Mitscher, L. A.; et al. *J. Antibiot.* **1977**, 30, 552. (b) Okami, Y.; et al. *Ibid.* **1979**, 32, 964. (c) Deushi, T.; et al. *Ibid.* **1979**, 32, 187.

(5) For the synthesis of a derivative of (\pm)-**2a** from myoinositol and its use in the synthesis of fortimicin B, see: Honda, Y.; Suami, T. *Bull. Chem. Soc. Jpn.* **1982**, 55, 1156.

(6) Conduritol isolation: (a) Kubler, K. *Arch. Pharm. Ber. Stsch. Pharm.* **1908**, 246, 620. (b) Manni, P. E.; Sinsheimer, J. E. *J. Pharm. Sci.* **1965**, 54, 1541.

(7) Conduritol synthesis (nonstereospecific): Nakajima, M.; Tomida, I.; Takei, S. *Chem. Ber.* **1957**, 90, 246.

(8) Compound **4** was prepared by reaction of the sodium salt of anthrone (NaH, THF, 25 °C) with (benzyloxy)methyl chloride.

(9) Gemal, A. L.; Luche, J.-L. *J. Am. Chem. Soc.* **1981**, 103, 5454.

(10) VanRheenen, V.; Kelly, R. C.; Cha, D. Y. *Tetrahedron Lett.* **1976**, 17, 1973.